Supporting Information:

Molecular Dynamic Simulation Insights into the Cellular Uptakes of Elastic Nanoparticles through Human Pulmonary Surfactant

Akkaranunt Supakijsilp,[†] Jing He,[†] Xubo Lin,[‡,] and Jian Ye[†,ϕ,*]*

[†]School of Biomedical Engineering, Shanghai Jiao Tong University, Shanghai 200030, P. R. China

[‡]Beijing Advanced Innovation Center for Biomedical Engineering, School of Engineering Medicine, Beihang University, Beijing 100191, P. R. China.

[ϕ]Institute of Medical Robotics, Shanghai Jiao Tong University, Shanghai 200240, P.R. China

*To whom correspondence should be addressed. E-mail: yejian78@sjtu.edu.cn; linxbseu@buaa.edu.cn

1. The information of the control system

The simulation results in both active and passive cellular uptake pathways of the control system composed of saturated dipalmitoyl phosphatidyl-choline (DPPC), unsaturated dioleoyl phosphatidyl-choline (DOPC), and cholesterol (CHOL) in a ratio of 5:3:2 is shown in **Figure S1-2**. The total simulation runtime is 170 ns at body temperature (310 K).

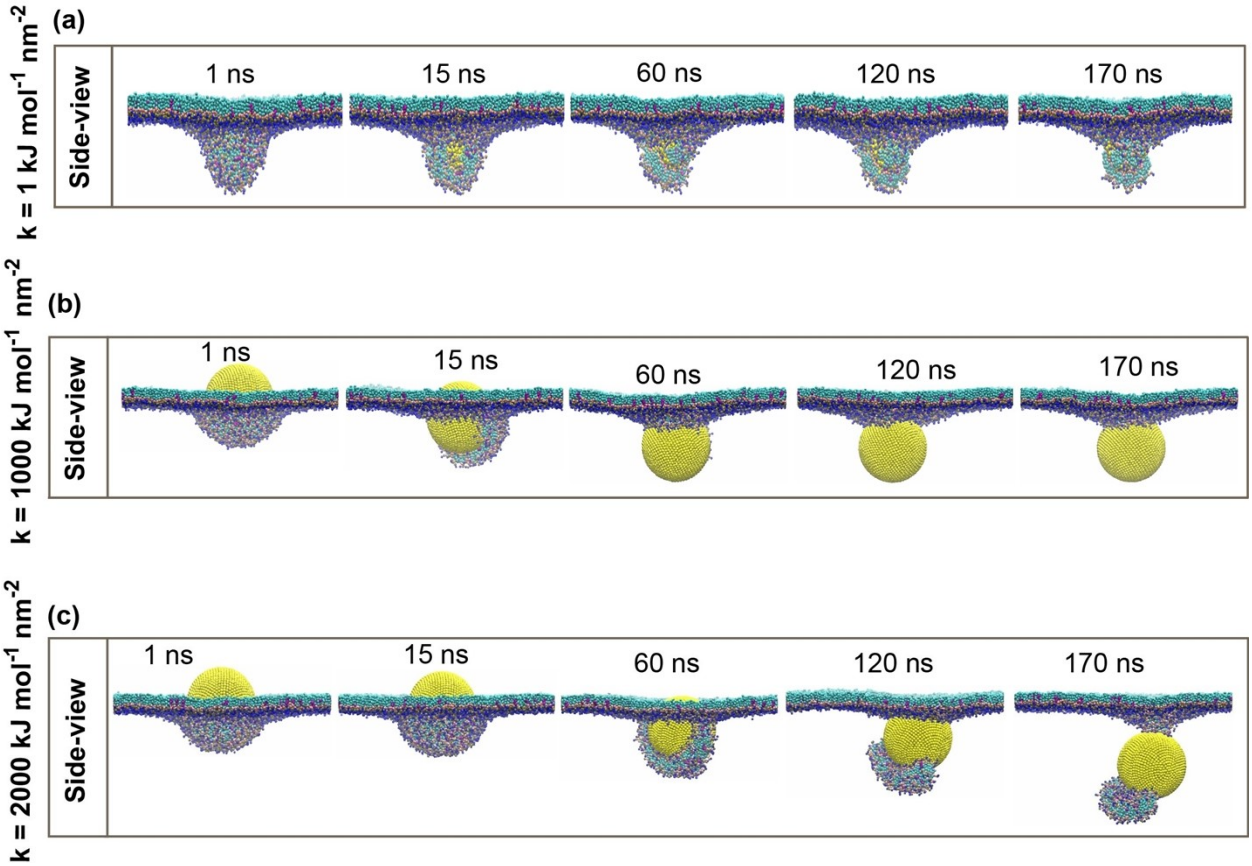

Figure S1. Simulation results of the control system with active cellular uptake pathway. (a) The soft CG-NP with spring constant (k) equal 1 kJ mol^{-1} nm^{-2}, (b) intermediate CG-NP with spring constant (k) equal 1000 kJ mol^{-1} nm^{-2}, and (c) stiff CG-NP with spring constant (k) equal 2000 kJ mol^{-1} nm^{-2}. Water and ions have been removed for greater visualization.

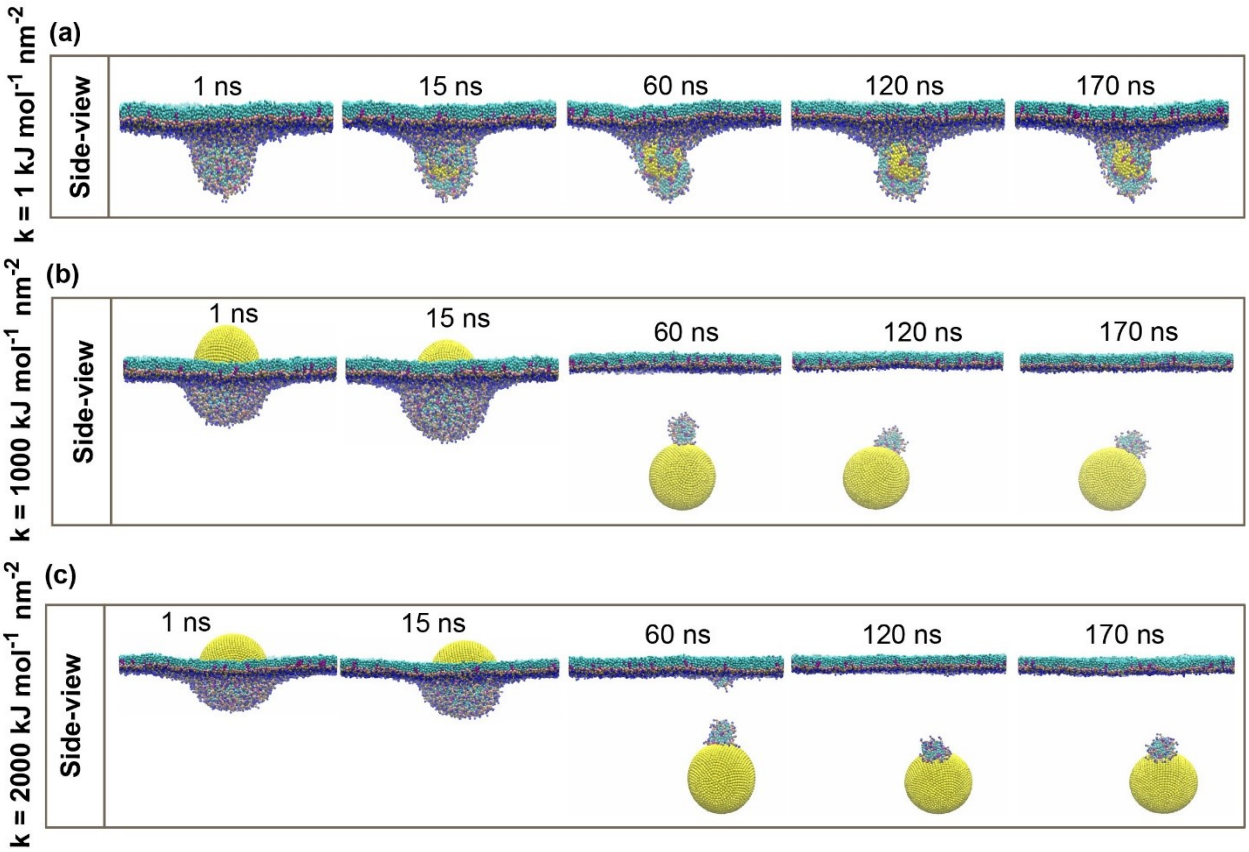

Figure S2. Simulation results of the control system with passive cellular uptake pathway. (a) The soft CG-NP with spring constant (k) equal 1 kJ mol^{-1} nm^{-2}, (b) intermediate CG-NP with spring constant (k) equal 1000 kJ mol^{-1} nm^{-2}, and (c) stiff CG-NP with spring constant (k) equal 2000 kJ mol^{-1} nm^{-2}. Water and ions have been removed for greater visualization.

2. The simulation results of the repeated simulations

The additional simulation repeats of both active and passive settings for all three elastic NPs were performed. All the simulation parameters and runtime are identical for each of the previous results. The repeated simulation runs are used to support the penetrability of all elastic NPs types.

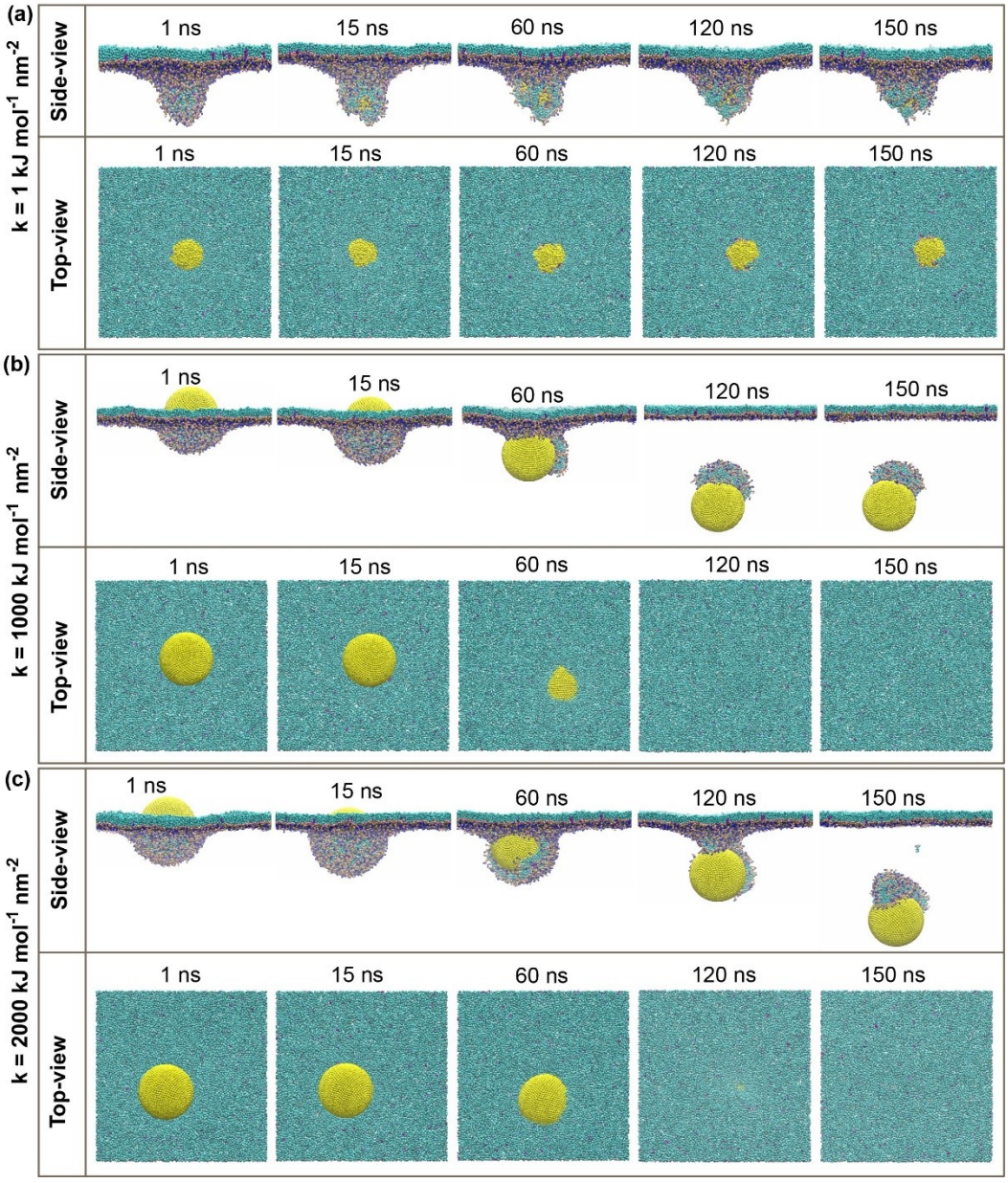

Figure S3. Simulation repeats of active cellular uptake. (a) The soft CG-NP with spring constant (k) equal 1 kJ mol^{-1} nm^{-2}, (b) intermediate CG-NP with spring constant (k) equal 1000 kJ mol^{-1} nm^{-2}, and (c) stiff CG-NP with spring constant (k) equal 2000 kJ mol^{-1} nm^{-2}. Water and ions have been removed for greater visualization.

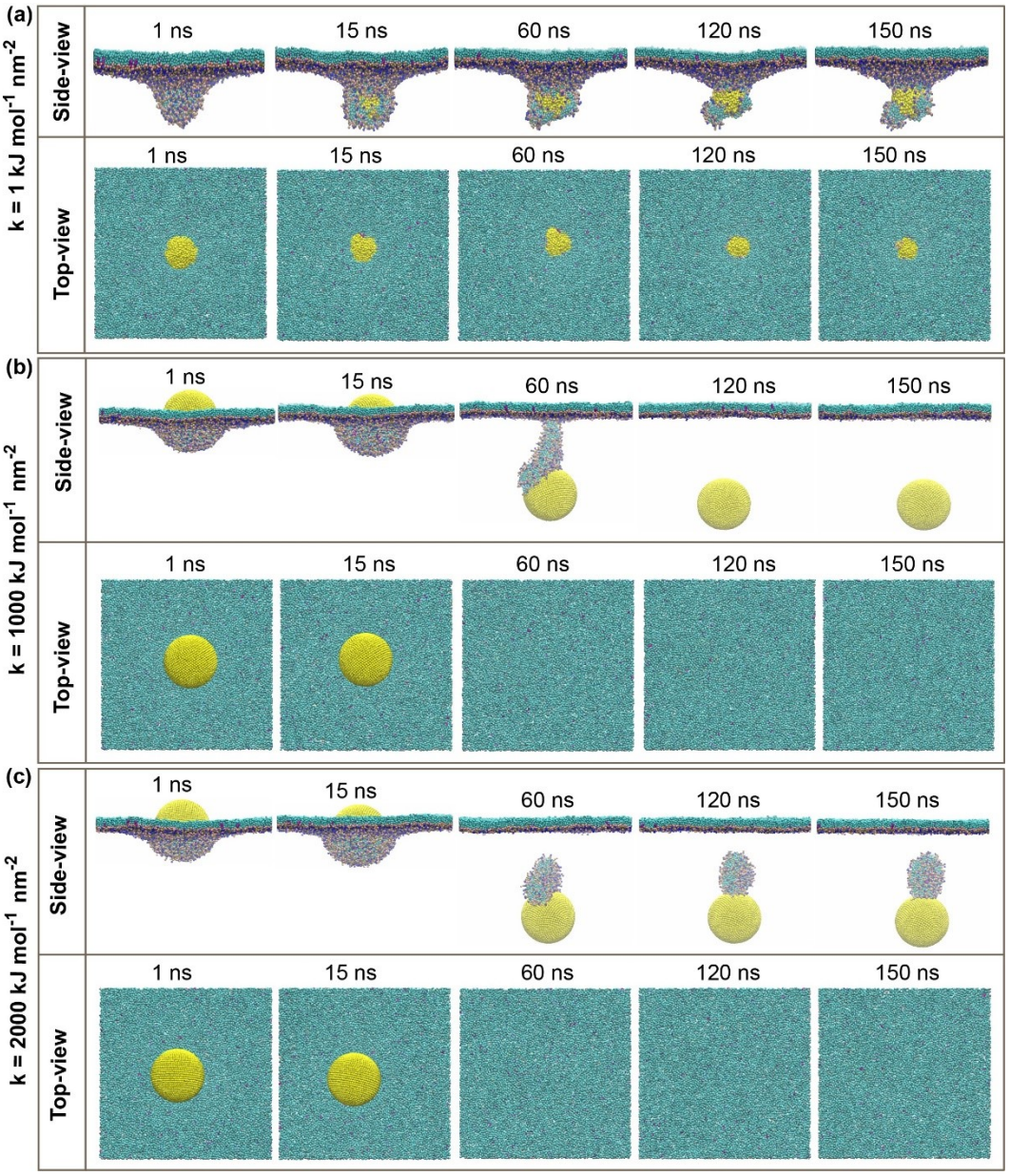

Figure S4. Simulation repeats of passive cellular uptake. (a) The soft CG-NP with spring constant (k) equal 1 kJ mol^{-1} nm^{-2}, (b) intermediate CG-NP with spring constant (k) equal 1000 kJ mol^{-1} nm^{-2}, and (c) stiff CG-NP with spring constant (k) equal 2000 kJ mol^{-1} nm^{-2}. Water and ions have been removed for greater visualization.

3. The Voronoi diagram of Area Per Lipid

Voronoi diagram of APL in active/passive cellular uptake using APL@Voro. In APL, NPs with pulmonary surfactant (PS) monolayer contacts are displayed in black polygons, and the pure NPs are shown in white polygons. The different colors of the Voronoi diagram indicate the diverse range of APL values respected to the left-hand side color bar.

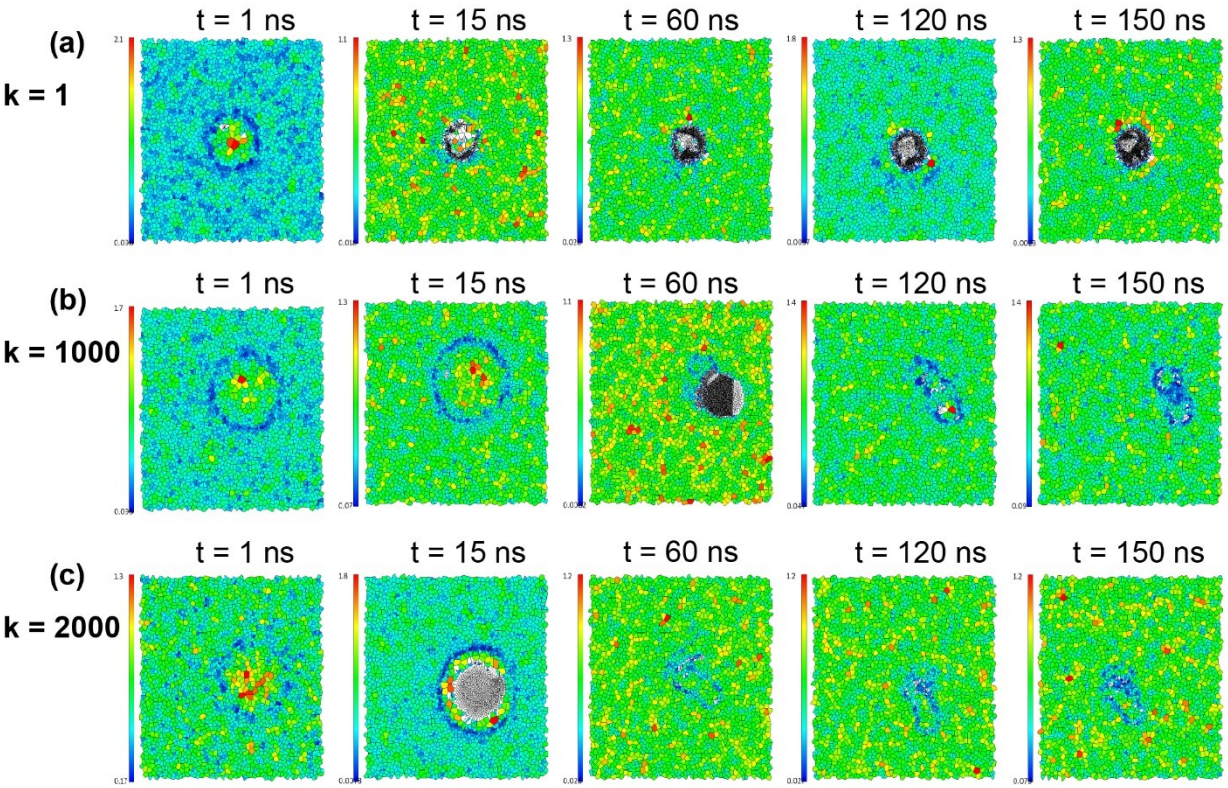

Figure S5. Voronoi diagram of APL for active cellular uptake generated from APL@Voro.

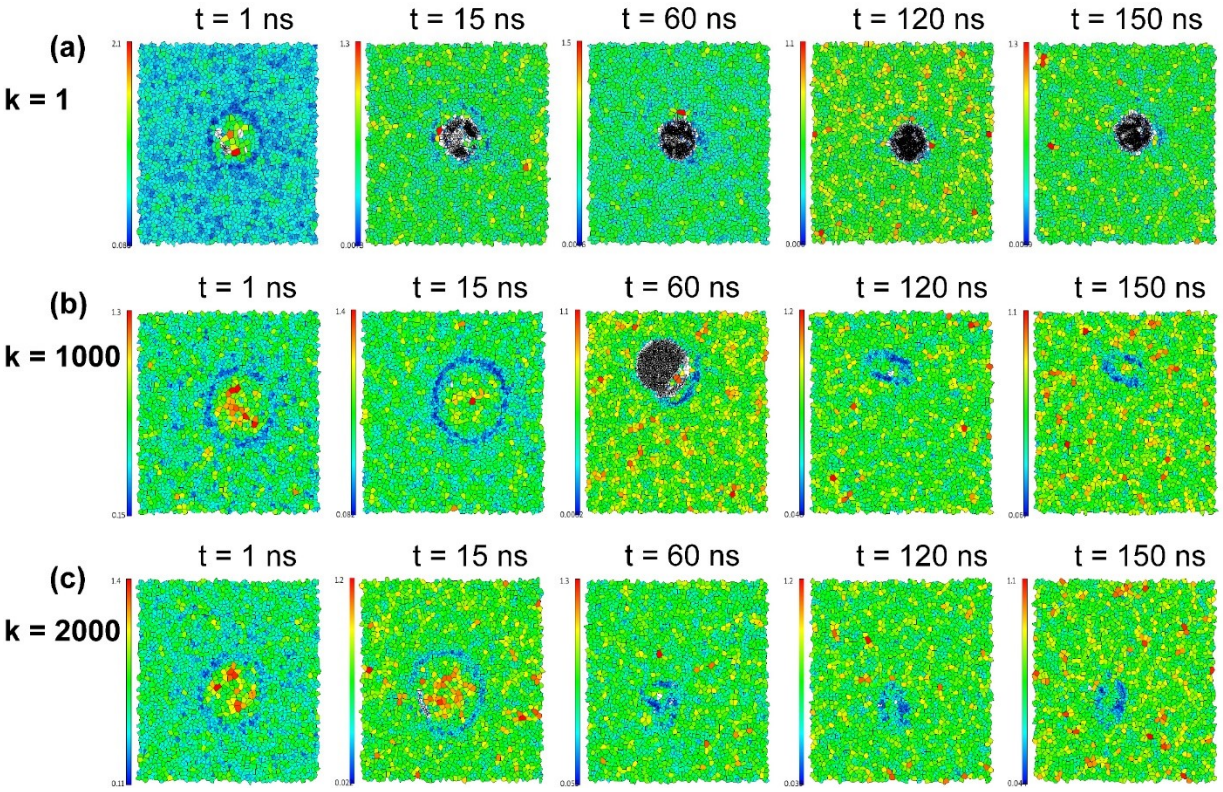

Figure S6. Voronoi diagram of APL for passive cellular uptake generated from APL@Voro.

4. Snapshot of CG-NP Partial Density

The partial density profile of three NP types shows the relationships between the difference value of spring constant (k) and the partial density of the NP, as shown in **Figure S7**. The partial density profile of active/passive cellular uptake has been compared. Dot lines represent active cellular uptake, while straight line represents passive cellular uptake. The partial density shows a directly proportional relationship with the spring constant (k) value. The soft NP has the lowest partial density, followed by the intermediate and the stiff NP which is corresponding to k = 1, 1000 and 2000 kJ mol^{-1} nm^{-2}, respectively.

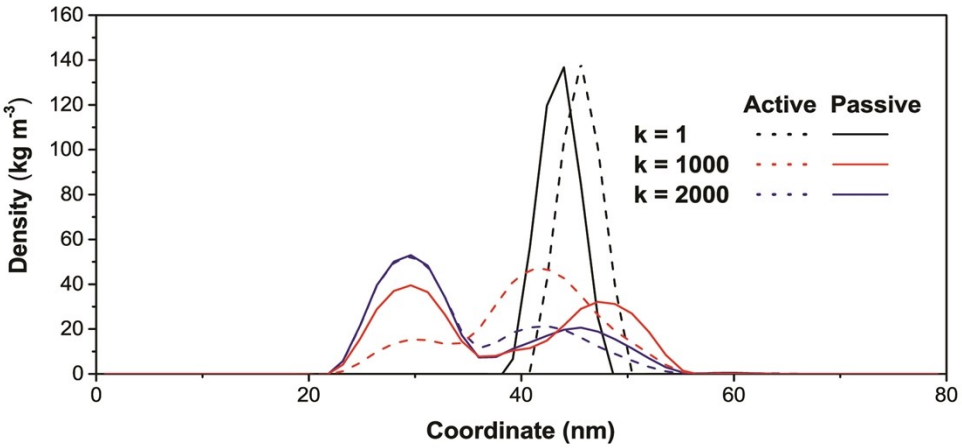

Figure S7. Snapshots of partial density plots for all three NP types throughout the total simulation runtime have been shown. Dot lines represent active cellular uptake, and the solid line represents passive cellular uptake.

5. Lipid Order Parameter

The lipid order parameter explains the C-H bond vector orientation of the bilayer normal Z within all the sampling time and was calculated using the following formula:

$$S_{CH} = \frac{\langle 3\cos\theta - 1 \rangle}{2}$$

Where θ is the angle between the bond and the bilayer normal.

Lipid order parameter (S_{CH}) calculations for the entire simulation time of 150 ns have been calculated to investigate the effect of contact area caused by NPs-induced deformation. S_{CH} shows the lipids structuring order inside the PS monolayer. A value of -0.5 indicates a perfect anti-alignment orientation of the lipid tails, 0 indicates a random distribution, and 1 shows the perfect alignment orientation of the lipid tails. The lipid order parameter S_{CH} for PS monolayer is obtained as a function of the number of carbon atom and the lipid tails for both active and

passive cellular uptake pathways, as shown in **Figure S8**. In both active and passive cellular uptake cases, all types of NPs have caused the S_{CH} value to deviate dramatically from the non-NPs system (pink line) for all lipid types, namely DPPC, POPG and CHOL. The significant difference of active and passive cellular uptakes for DPPC and POPG (**Figure S8a, Figure S8b, Figure S8d and Figure S8e**) is in passive cellular uptake. The effects of elasticity modification do not possess any difference between the three types of NP as all the plots are overlapped, while for active cellular uptake the soft NP (black line) is having the highest S_{CH} follows by the stiff and intermediate NPs (blue and red line). For CHOL **(Figure S8c and Figure S8f)**, in both active and passive cellular uptake cases, all the plots tend to overlap. There is a slight difference in the intermediate NP (red line) which is lower than the overlapped plots of the soft and the stiff NPs (black and blue line) in the active cellular uptake, on the other hand in passive cellular uptake, all plots have the same trend, but the intermediate NP (red line) plots show slightly higher than the soft and stiff NPs (black and blue line).

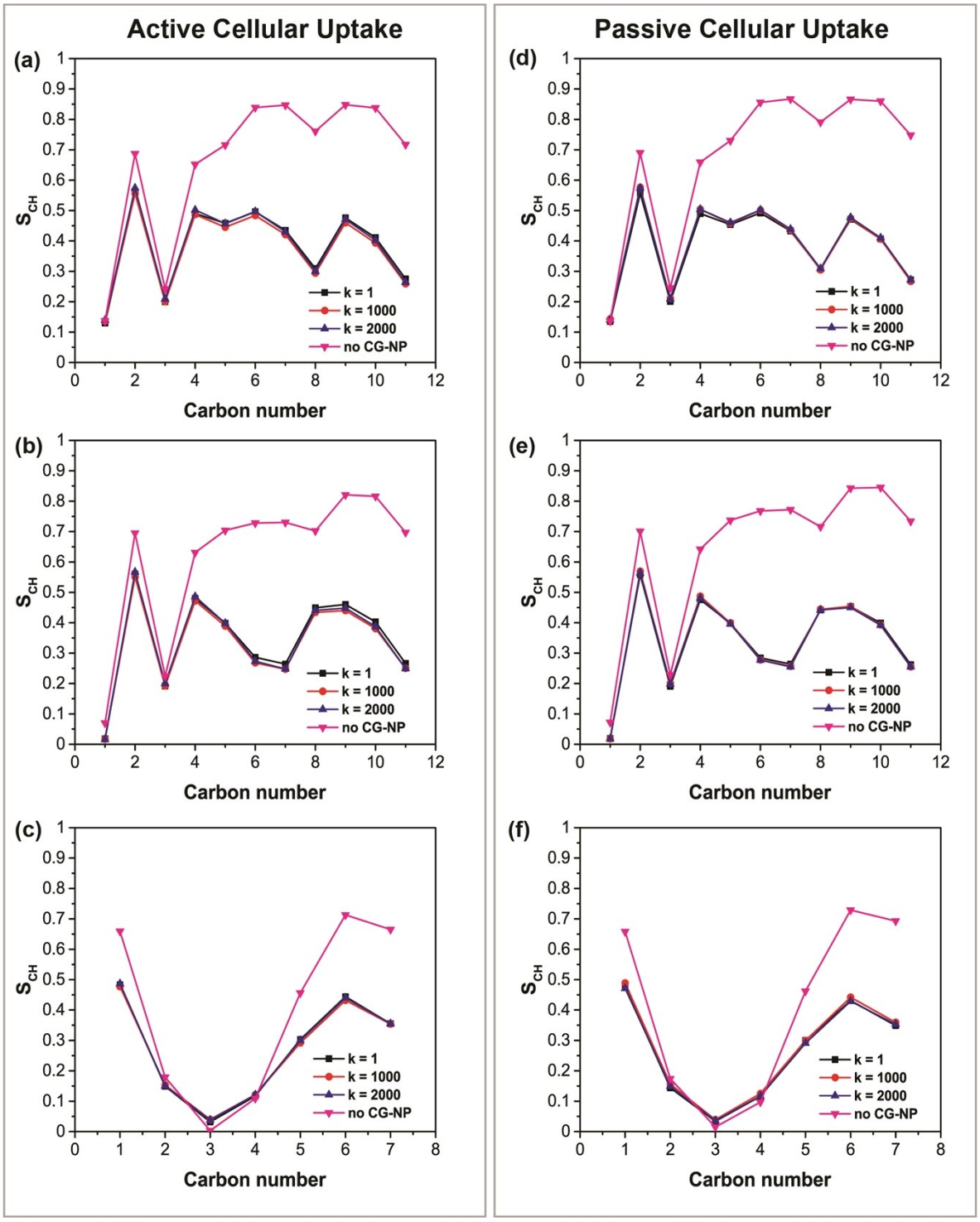

Figure S8. Snapshots of lipid order parameter variation for the systems of active/passive cellular uptake. (a-c) Consecutively, interpretation of DPPC, POPG, and CHOL in active cellular uptake settings. (d-f)

interpretation of DPPC, POPG, and CHOL in passive cellular uptake settings, respectively. The lipid order parameter profiles were calculated over the last 150 ns.